Cite this article as: Kumar, P., Fennell, P., Symonds, J., Britter, R., 2008. Treatment for the losses of aerosol particles in long sampling tubes during ambient particle measurements. Atmospheric Environment 42, 8819–8826.

# Treatment of losses of ultrafine aerosol particles in long sampling tubes during ambient measurements

**Prashant Kumar[a*], Paul Fennell[b], Jonathan Symonds[c] and Rex Britter[a]**

[a]*Department of Engineering, University of Cambridge, Cambridge CB2 1PZ, UK*
[b]*Department of Chemical Engineering, Imperial College London, London SW7 2AZ, UK*
[c]*Cambustion Ltd., J6 The Paddocks, Cambridge CB1 8DH, UK*

## Abstract

Long sampling tubes are often required for particle measurements in street canyons. This may lead to significant losses of the number of ultrafine (those below 100 nm) particles within the sampling tubes. Inappropriate treatment of these losses may significantly change the measured particle number distributions (PND), because most of the ambient particles, by number, exist in the ultrafine size range. Based on the Reynolds number ($R_e$) in the sampling tubes, most studies treat the particle losses using the Gormley and Kennedy (1949) laminar flow model or the Wells and Chamberlain (1967) turbulent flow model. Our experiments used a particle spectrometer with various lengths (1.00, 5.47, 5.55, 8.90 and 13.40 m) of sampling tube to measure the PNDs in the 5–2738 nm range. Experiments were performed under different operating conditions to measure the particle losses through silicone rubber tubes of circular cross–section (7.85 mm internal diameter). Sources of particles included emissions from an idling diesel engine car in a street canyon, emissions from a burning candle and those from the generation of salt aerosols using a nebuliser in the laboratory. Results showed that losses for particles below ≈20 nm were important and were largest for the smallest size range (5–10 nm), but were modest for particles above ≈20 nm. In our experiments the laminar flow model did not reflect the observations for small $R_e$. This may be due to the sampling tubes not being kept straight or other complications. In–situ calibration or comparison appears to be required.

***Keywords:*** Aerosol deposition, Particle diffusion losses; Particle number distribution; Street canyon; Ultrafine particles

[*] Corresponding author, Department of Engineering, University of Cambridge, Cambridge CB2 1PZ, UK; Tel.: +44–(0)1223 332681; Fax: +44–(0)1223 332662. Email addresses: pp286@cam.ac.uk or pp286@rediffmail.com (Prashant Kumar), rb11@cam.ac.uk (Rex Britter).

## 1. Introduction

In many studies of ambient aerosols, experimental conditions force the use of long sampling tubes when commonly deployed instruments such as the Scanning Mobility Particle Sizers (SMPS), the Electrical Low Pressure Impactor (ELPI), the Aerodynamic Particle Sizer (APS) or the Differential Mobility Spectrometer (DMS500) are used for measuring particle number distributions (PND) and/or particle number concentrations (PNC). These studies include a recent experimental campaign (Kumar et al., 2008a–d) where a fast response differential particle spectrometer (DMS500) measured the PNDs at the roadside. Losses of ultrafine (those below 100 nm) particles inside the sampling tubes were observed, with smaller particles suffering greater losses. Correction for these losses (by number but not by mass) is critical since most of the ambient particles, by number, exist in the size range (below 100 nm) where these losses are also the largest (Kumar et al., 2008b). Based on the Reynolds number in the sampling line, several studies (Agus et al., 2007; Kumar et al., 2008a; Kumar et al., 2008c; Lingard et al., 2006) treat particle losses in straight tubes using either the Gormley and Kennedy (1949) laminar model or the Wells and Chamberlain's (1967) turbulent model. Unfortunately, only a few studies discuss the importance of such losses (Noble et al., 2005; Symonds et al., 2007a; Wang et al., 2002). Noble et al. (2005) measured particles in a continuous field measurement for laminar flow conditions in sampling tubes using a SMPS and an APS through a 3 m long aluminium tube (2.54 cm internal diameter) that was vertically oriented with slight bends for connections to the sampling instruments. They reported that the penetration efficiency was substantially smaller than the theoretical penetration efficiency for both ultrafine and fine particles. Similarly, Symonds et al. (2007a) reported that the penetration efficiency of particles in the 5–100 nm range for sampling tubes up to 25 m long, made of silicone rubber, was much closer to the turbulent flow model even though the

Reynolds number indicated laminar flow. Wang et al. (2002) reported the effect of bends and elbows on diffusion of mono disperse particles (5–15 nm) for a range of Reynolds numbers (80–950). They concluded that in a flow passage with four elbows, each having 90° bends, the penetration efficiency was up to 44% smaller than for a straight tube of same length. However, particle losses and their appropriate treatment for different length of sampling tubes, as would typically be used in ambient aerosol studies, need further attention.

In this study, a DMS500, with a four–way switching system, measured the PNDs in a broad (5–2738 nm) size range, pseudo–simultaneously. Various lengths of sampling tubes, between 1 and 14 m, made of silicone rubber, having 7.85 mm internal diameter (i.d.), were used to measure the particle penetration efficiencies. Three different and continuous sources of particles were used: an idling diesel–engined car in a street canyon, a burning candle and salt aerosols from a nebuliser (PARI LC+) in the laboratory.

The aim of the study was to investigate particles losses in sampling tubes of various lengths under different operating conditions of the DMS500. The experimental results are compared with particle loss models for laminar and turbulent flow and it is shown that such losses are extremely important for the ultrafine particles that are dominant (by number) in the urban environment (Kumar et al., 2007, 2008a–d; Longley et al., 2003).

## 2. Methodology

### 2.1 Theories of particle losses in sampling line

There are five main mechanisms which may lead to particle losses on to the surface of a sampling tube; these are sedimentation (gravitational), thermophoresis, electrostatic, inertial impaction and diffusion (Friedlander, 2000; Hinds, 1999; Ketzel

and Berkowicz, 2004). Of all potential losses, those due to diffusion and inertial impaction are most important for ambient particle measurements (Hinds, 1999). The second of these is only important under turbulent flow conditions and for particles larger than 100 nm (Lee and Gieseke, 1994). Gormley and Kennedy (1949) first derived the equation for diffusional losses in a fully developed laminar flow (Reynolds number, $R_e$<2300) through a tube of circular cross section (diameter $d_t$) with a uniform inlet PNC, as a function of a dimensionless deposition parameter $\beta = 4DL/\pi d_t^2 \overline{U}$, where $D$ is the diffusion coefficient (see supplementary Section S.1 for details), $L$ is the tube length and $\overline{U}$ is the average flow velocity through the tube. A simplified version of a more complicated and more accurate expression (Hinds, 1999), gives penetration efficiency $P$, which is the fraction of entering particles ($N_{in}$) that exit ($N_{out}$) through a tube, with an accuracy of 1% for all values of $\beta$ to be:

$$P = N_{out}/N_{in} = 0.819e^{-11.5\beta} + 0.0975e^{-70.1\beta} \quad \text{for } \beta \geq 0.009 \quad (1a)$$

$$P = N_{out}/N_{in} = 1 - 5.50\beta^{2/3} + 3.77\beta \quad \text{for } \beta < 0.009 \quad (1b)$$

For straight sampling tubes, Ramamurthi et al. (1990) confirmed the accuracy of the above equations during their study that used radioactive $^{218}PoO_x$ aerosol clusters through a 2.2 cm i.d. tube of various lengths (i.e., 88 mm, 205 mm and 317 mm). Their work was supported by Alonso et al. (1997) for particles down to 2 nm diameter by analysis of the penetration efficiencies of nanometre–sized aerosol particles through a plastic tube of 10 mm i.d.

Under turbulent pipe flow conditions ($R_e$>2300), the deposition onto tube surfaces is more complicated and equations describing it cannot be solved explicitly. Assuming that turbulent flow provides a constant concentration everywhere beyond a thin boundary layer next to the surface of the tube walls where the flow is laminar and the concentration decreases linearly from constant to zero at the surface walls, Wells

and Chamberlain (1967) gave an expression for diffusive deposition velocity ($V_d$) through the laminar sub–layer for turbulent flow in a tube as:

$$V_d = \frac{0.04\overline{U}}{R_e^{1/4}}\left(\frac{\rho_g D}{\eta}\right)^{2/3} \quad (2)$$

where $\rho_g$ and $\eta$ are the density and the viscosity of fluid passing through the tube. Using the deposition velocity (as given in Eq. 2), Lee and Gieseke (1994) presented an empirical equation for the overall penetration through a tube of length $L$ subjected to losses to the walls by diffusion and inertial impaction from turbulent flow as:

$$P = \frac{N_{out}}{N_{in}} = \exp\left(\frac{-4V_d L}{d_t \overline{U}}\right) \quad (3)$$

Eq. (3) also includes inertial deposition but this is only significant for particles larger than around 100 nm.

## 2.2 Instrumentation

A four–way solenoid switching system was used with a fast response differential mobility spectrometer (Cambustion DMS500) to measure the particle number and size distributions in 5–2738 nm size range through different lengths of tube pseudo–simultaneously. Cylindrical sampling tubes of 7.85 mm i.d. and various lengths, $L_{\text{base}}$ (1.00 m), $L_1$ (5.47 m), $L_2$ (5.55 m), $L_3$ (8.90 m) and $L_4$ (13.40 m), were used to analyse the particle losses inside the electrically conductive sampling tubes that were made of silicone rubber. As seen in Fig. 1, there were two parts to the switching system, namely a stainless steel manifold having one inlet and four outlets, and a four–way solenoid switching system. A steel funnel was fixed at the head of steel manifold inlet. The outlets of the manifold were connected to cyclones by small pieces of rubber sampling tubes. The cyclones were then connected to the four–way switching system by another piece of silicone rubber sampling tube; the length of these small connecting

sections is included in above–mentioned tube lengths $L_{base}$, $L_1$, $L_2$, $L_3$ and $L_4$. Finally, the four–way switching system was connected to the DMS500, as seen in Fig. 1. The cyclones prevent large particles entering the sampling tube and the instrument. All the sampling tubes were laid horizontally on the ground but small bends were present due to the difference in height between the instrument and the emission sources of particles.

The DMS500 used is capable of measurements over two size ranges (i.e., 5–1000 nm and 5–2738 nm). Each of these ranges requires different set–points for the instrument's internal flows, voltages and pressure. The use of these two ranges in these experiments enabled two different sample flow rates and pressures to be examined (discussed in detail in Section 3.2). To measure the PNDs in the 5–1000 nm range, steel restrictors with holes of ≈1.00 mm i.d. were placed upstream of the cyclones to maintain a flow rate of 8 standard litres/min (slpm) and a pressure of 0.25 bar (the same as the instrument's classification column) inside the sampling tube. However, the instrument could also be used to measure PNDs in the 5–2738 nm range, when restrictors of 0.5 mm i.d. were substituted for the 1.00 mm ones, maintaining a flow rate of 2.5 slpm and pressure 0.16 bar inside the sampling tube (the classifier operates at lower pressure to achieve the increased electrical mobility size range). The orifice plates (a) reduce the pressure inside the sampling tubes hence reducing the likelihood of particle agglomeration, (b) set the sample flow rate to that required by the instrument, and (c) improve the time response of the instrument.

## 2.2 Measurements

Three different sources for nearly steady–state emissions were selected to measure the particle losses through the different lengths of sampling tubes. Exhaust emissions from a stationary diesel engine car at idle (Model: Rover 25 TD) in a street canyon (500 mm from the tail pipe) mimicked real field (i.e., operational) conditions. To verify these results, further experiments were replicated in the laboratory (i.e.,

controlled) conditions using particle emissions from a burning tea light candle and salt aerosols generated by a nebuliser (Pari LC+) at two different pressures (0.5 and 2.0 bar) to change the aerosol concentration. The details of the use of this nebuliser to generate salt aerosols have been described elsewhere (Fennell et al., 2007). The tea light candle consisted circular plugs of paraffin wax (37 mm diameter and 15 mm high) in a thick aluminium casing (Daeid and Thain, 2002). The DMS500 measures particles based on electrical mobility equivalent diameter (hereafter called as $D_p$) that implicitly takes into account the characteristics of aerosols (i.e., shape, surface area, charge etc.). The different types of particle sources were found not to influence the particle losses in this study, as is discussed later in Section 3.2 (Figs. 3–5) where experimental data from all sources show similar penetration efficiency for a particular particle diameter. This is because the equations governing losses of particles (see Section S.1 in supplementary material) are based on the aerodynamic mobility diameter, which is very close to $D_p$, so that differences between different aerosols are explicit in the models. Measurements were taken at a sampling frequency of 0.5 Hz, rather than the maximal frequency of 10 Hz to improve the signal–to–noise ratio, continuously for 1–min in each tube length. These were repeated for four complete cycles (i.e. four × 1–min measurements for each tube length taken on four different occasions). Further details of the experiment and the operating conditions are shown in Table 1.

## 3. Results and Discussion

### 3.1 Effect of tube length on particle number distributions

To derive the losses in the sampling tubes, it is assumed that the losses in $L_{base}$ are equivalent to the losses in the first metre of each of other four tubes, and subsequent losses are determined in each tube relative to their "corrected" length (i.e., their actual length minus 1 m). The size dependent penetration efficiencies for the effective length

of different tubes were then defined as the number concentration through the effective lengths $L_1$, $L_2$, $L_3$ and $L_4$ of tube divided by the number concentration penetrating $L_{base}$. Fig. 2 shows the effect of various length of sampling tubes on particulate emissions from a diesel–engined car. As the tube lengths increases from $L_{base}$ to $L_4$, the magnitude of the PNDs decreased. The PNDs in smaller size range (below ≈20 nm) showed larger changes, indicating relatively greater losses of particles with increased length of sampling tubes. However, the PNDs above ≈20 nm showed negligible changes, indicating modest particle loss. The PNCs, which were obtained by integrating the PND profiles seen in Fig. 2, decreased about 3, 7, 28 and 32% for $L_1$, $L_2$, $L_3$ and $L_4$, respectively, with reference to $L_{base}$. It should be noted that the majority of the decrease in PNC was for particles below ≈20 nm where the maximum losses are also expected due to the higher diffusivity of smaller particles. For example, penetration efficiencies for $L_4$ were observed to be ≈10% for 5 nm diameter, ≈40% for 10 nm diameter, and well above 60% for particles in the 10–20 nm size range. Other sources also showed similar trend for penetration efficiencies, as can be seen from Figs. 3–5.

### 3.2 Effect of operating conditions on the size–dependent penetration of particles in various tube lengths

Size–dependent penetration efficiencies of particles in $L_2$, $L_3$ and $L_4$ for all cases described in Table 1 are shown in Figs. 3, 4 and 5, respectively. The penetration efficiencies shown in these figures are estimated based on the PNCs which were averaged over the time period of four complete cycles as mentioned in Section 2.2. Particle emissions from various sources were nearly in steady–state conditions since the geometric mean diameter with standard deviation over the averaged periods were 13.7±0.7, 12.5±0.5 and 10.2±0.8 nm for car emissions, salt aerosols and candle emissions, respectively. Tube length $L_1$ is not considered for further analysis since $L_1$ ≈

$L_2$. The results for $Car_2$ and $Car_3$ are generally similar with the penetration efficiencies being similar to the theoretical "turbulent" flow model except for $Car_3$ with the longest sampling tube and for the larger particles. The candle results for all three sampling tube lengths also produce a similar result to the $Car_2$ and $Car_3$ result.

Sensitivity analysis of Eqs. (1–3) suggest that apart from the length of the sampling tubes, their diameter, sample flow rate or mean velocity (since both are linked), sample line pressure and temperature are variables affecting the particle losses in the sample line. The effect of different tube diameters on penetration efficiencies could not be seen because our experiments used only a fixed diameter tube. The effect of sample line temperature (assumed to be equal to ambient temperature) on penetration efficiencies seem to be modest for our conditions. This can be seen by the comparison of Figs. 3a, 4a and 5a (for 8.2 °C) with Figs. 3b, 4b and 5c (for 26 °C), respectively, where all other conditions were similar except temperature (see Table 1). For instance, the average of the modelled penetration efficiency in the 5–100 nm size range for $L_2$ showed fractional changes; ≈89% for 8.2 °C as compared with ≈88.8% for 26 °C, as seen in Figs. 3a and 3b. However, this difference was larger for experimental results where the average penetration efficiencies were ≈78% for 8.2 °C as compared with ≈73% for 26 °C.

When using the DMS500, the sample line pressure and the sample flow rate are not independent variables, due to the requirement for 8 slpm when 0.25 bars is used, or 2.5 slpm with 0.16 bars. Considering our experimental conditions (as explained in Table 1 for different cases) the sample flow rate was identical (2.5 slpm) for the first four cases, and these cases are averaged and shown in part (d) of each of Figs. 3–5 whereas this was 8 slpm for the last two cases, as seen in Table 1 and in part (c) of Figs. 3–5. Comparison of Figs. 3c, 4c and 5c with Figs. 3d, 4d and 5d, respectively,

indicate the effect of change in the sample flow rate on the measured and modelled results. As expected from the sensitivity analysis, the penetration efficiencies for modelled results for all lengths of sampling tubes were consistently larger for 8 slpm sample flow rate (Figs. 3c, 4c and 5c) than for 2.5 slpm sample flow rate (Figs. 3d, 4d and 5d) since the diffusive deposition velocity, as seen in Eq. (2), increases considerably with increased sample flow rate. For example, the average of the modelled penetration efficiency in the 5–100 nm size range for $L_2$ during laminar flow conditions was ≈93% for 8 slpm as compared with ≈88% for 2.5 slpm, as seen in Figs. 3c and 3d. Surprisingly, this effect was not clearly distinguishable on the measured penetration efficiencies which were much smaller (and nearly similar for both sample flow rates) than those for modelled penetration efficiencies for laminar flow conditions; ≈74% for 8 slpm as compared with ≈73% for 2.5 slpm. Moreover, the average of the measured penetration efficiencies in the 5–100 nm size range was found to be closer to those for the turbulent flow model, where these were ≈60% for 8 slpm than ≈54% for 2.5 slpm. The reasons for this are discussed in Section 3.3. Similar observations were found for other lengths ($L_3$ and $L_4$) of the sampling tubes, as can be seen from Figs. 4–5.

Further investigation of the measured results showed that particle losses are very significant between 5 and 10 nm for all cases (Figs. 3–5); these are as high as ≈90% for 5 nm particles and ≈60% for 10 nm diameter. There is a sharp rise in penetration efficiency between 10 nm and 20 nm diameter. Above 20 nm diameter particle losses are modest.

### 3.3 Comparison of experimental results with laminar and turbulent flow diffusion models

Particle losses for various cases are compared below with diffusion models for

laminar (Hinds, 1999) and turbulent (Wells and Chamberlain, 1967) flow, which are represented by Eqs. (1) and (3), respectively. As shown in Table 1, flow conditions in the sampling tubes were laminar ($R_e$ = 461 and 1409) during all the experiments. For all cases, particle losses were substantially larger for the experimental results than for modelled results calculated for laminar flow, as seen in Figs. 3–5. Interestingly, all the cases presented in Figs. 3, 4 and 5 for $L_2$, $L_3$ and $L_4$, respectively, show that measured penetration efficiencies for particles below ≈20 nm diameters are generally closer to the modelled diffusion losses for turbulent flow. Conversely, the measured penetration efficiencies for particles above ≈20 nm indicated modest particle losses, but part (d) of Figs. 3–5, interestingly, shows that the measured penetration efficiencies are closer to the modelled penetration efficiencies for the laminar flow; no clear explanation for this similarity was found. Particle losses below ≈20 nm only are discussed further in this article.

As discussed in Section 2.1, studies for short and straight tubes (Alonso et al., 1997; Ramamurthi et al., 1990) confirmed the laminar flow model under conditions commonly found *within* aerosol instruments. Conversely, when relatively longer sampling tubes are used, particle losses where laminar flow is expected have been found to be considerably larger than the modelled losses for laminar flow conditions (Wang et al., 2002; Noble et al., 2005; Symonds et al., 2007), as is confirmed by our brief study. The present study tested these findings for various operating conditions and for different lengths of sampling tubes ranging from 1 to 14 m, as described in Table 1. It might be expected that losses greater than those which are predicted by the model could result from other mechanisms such as in the connections to the switching system. However, these can be neglected here since they are common to all sampling tubes.

Prediction of particle penetration efficiencies is not straightforward since they depend on the complex flow field inside the tubes. It is probable that non–straightness

(or small bends) in the sampling tubes will produce secondary flows, and intermittent enhanced movement of the particles towards the sampling tube walls. These flow conditions can also occur due to any roughness in the inner–walls of the sampling line; however, this effect will be relatively small and can be ignored (Pope, 2003). The evidence of the presence of secondary flow can be supported by arguments based on the Dean number (De). The strength of secondary flow produced by flow through a smooth bend of radius $R$ can be represented by $De = R_e (d_t/2R)^{0.5}$; where $d_t$ is the tube diameter (Pui et al., 1987). An increase in De will increase the strength of the secondary flow (Tsai and Pui, 1990), suggesting that for a fixed tube diameter an increase in angle of bend decreases the bend radius and increases De. For example increasing the angle of bend from 45° to 90° reduces the radius of bend by ≈31% and increases De by ≈13%. This suggests that an increase in angle of bend could result in much smaller particle penetration efficiencies than expected during laminar flow conditions. Furthermore, change in diameter of the sampling tubes is equally important for changing the De. For example, an increase in tube diameter from 7.85 mm to 10 mm (≈22%) decreases $R_e$ by ≈22%, resulting in a decrease of ≈11% in De; however our experiments were limited to sampling tubes of fixed diameter.

The presence of secondary flow in sampling tubes is further substantiated by the fact that the measured penetration efficiencies are closer to the modelled penetration efficiencies from Wells and Chamberlain's (1967) expression (Eq. 3) that takes in to account the diffusion of particles under turbulent flow conditions.

The above arguments suggest that an individual lay–out and diameter of a longer sampling tube are important aspects for changing the flow conditions. Consequently, in–situ calibration of the particle penetration is likely to be essential for the appropriate treatment of particle losses, though our results show that this can be

conducted in the laboratory, prior to any field campaign, since the size dependent penetration is similar for all aerosols investigated, in accordance with theory.

## 4. Summary and conclusions

Experiments were made under different operating conditions of the DMS500 particle spectrometer. Irrespective of any measured size range and different operating conditions used in various set of experiments, it was found that particle losses for particles smaller than ≈20 nm were important and needed to be taken into account when using long sampling tubes (>1 m). Maximal particle losses were found for particles between 5 and 10 nm, whereas losses were modest for particles larger than ≈20 nm. It can be concluded that ignoring these losses, especially below 20 nm (where a substantial number of the particles in ambient aerosols are to be found) may appreciably change the measured PNDs in the ambient environment. It was also apparent that even when the Reynolds number indicated that the flow was laminar, the turbulent penetration model of Hinds described particle losses best. Of course, it is most prudent to determine the losses of particles for any particular experimental setup directly.

This study presents preliminary results, and it would be interesting to perform similar experiments for different diameter of tubes and for various Reynolds numbers. More importantly, a study producing a thumb rule for angle of bends at which particle losses are minimum and/or are close to laminar flow model, will greatly benefit ambient aerosol studies.

## 5. Acknowledgements

Prashant Kumar acknowledges receipt of the Cambridge–Nehru Scholarship and the Overseas Research Scholarship Award for sponsoring his Ph.D. The authors thank Prof. A.N. Hayhurst and Dr. J.S. Dennis for the loan of the DMS500.

## 6. References


Alonso, M., Kousaka, Y., Hashimoto, T., Hashimoto, N., 1997. Penetration of nanometer–sized aerosol particles through wire screen and laminar flow tube. Aerosol Science and Technology 27, 471–480.

Agus, E. L., Young, D.T., Lingard, J.J.N., Smalley, R.J., Tate, E.J., Goodman, P.S., Tomlin, A.S., 2007. Factors influencing particle number concentrations, size distributions and modal parameters at a roof–level and roadside site in Leicester, UK. Science of the Total Environment 386, 65–82.

Daeid, N.N., Thain, E., 2002. Measurements of temperature rise over time for commercially available night lights (tea lights). Fire Safety Journal 37, 329–336.

Fennell, P.S., Dennis, J.S., Hayhurst, A.N., 2007. The sampling of nanoparticles of MgO formed when doping an oxygen–rich flame with magnesium. Combustion and Flame 151, 560–572.

Friedlander, S.K., 2000. Smoke, Dust and Haze: Fundamentals of Aerosol Dynamics, Oxford University Press, UK.

Gormley, P.G., Kennedy, M., 1949. Diffusion from a stream following through a cylinderical tube. Proceedings of Royal Irish Academy 52, 163–169.

Hinds, W.C., 1999. Aerosol technology: Properties, behaviour and measurement of airborne particles. John Wiley & Sons, UK.

Ketzel, M., Berkowicz, R., 2004. Modelling of the fate of ultrafine particles from exhaust pipe to rural background: an analysis of time scales for dilution, coagulation and deposition. Atmospheric Environment 38, 2639–2652.

Kumar, P., Fennell, P., Britter, R., 2007. Measurements and dispersion behaviour of particles in various size ranges (5 nm>dp<1000 nm) in a Cambridge street canyon Proceedings of the 11th International Conference on Harmonisation within Atmospheric Dispersion Modelling for Regulatory Purposes Cambridge, UK, pp. 368–372.

Kumar, P., Fennell, P., Britter, R., 2008a. Measurements of particles in the 5–1000 nm range close to road level in an urban street canyon. Science of the Total Environment 390, 437–447.

Kumar, P., Fennell, P., Langley, D., Britter, R., 2008b. Pseudo–simultaneous measurements for the vertical variation of coarse, fine and ultra fine particles in an urban street canyon. Atmospheric Environment 42, 4304–4319.

Kumar, P., Fennell, P.S., Hayhurst, A.N., Britter, R.E., 2008c. Street versus rooftop level concentrations of fine particles in a Cambridge street canyon. Boundary–Layer Meteorology (http://dx.doi.org/10.1007/s10546-008-9300-3).

Kumar, P., Fennell, P., Britter, R.E., 2008d. Effect of wind direction and speed on the dispersion of nucleation and accumulation mode particles in an urban street canyon. Science of the Total Environment 402, 82–94.

Lee, K.W., Gieseke, J.A., 1994. Deposition of particles in turbulent flow pipes. Journal of Aerosol Science 25, 699–704.

Lingard, J.J.N., Agus, E.L., Young, D.T., Andrews, G.E., Tomlin, A.S., 2006. Observations of urban airborne particle number concentrations during rush–hour conditions: analysis of the number based size distributions and modal parameters. Journal of Environmental Monitoring 8, 1203–1218.

Longley, I.D., Gallagher, M.W., Dorsey, J.R., Flynn, M., Allan, J.D., Alfarra, D., Inglish, D., 2003. A case study of aerosol (4.6nm<Dp<10μm) number and mass size distribution measurements in a busy street canyon in Manchester, U.K. Atmospheric Environment 37, 1563–1571.

Noble, C.A., Lawless, P.A., Rodes, C.E., 2005. A sampling approach for evaluating particle loss during continuous field measurements of particulate matter. Particle & Particle System Characterization 22, 99–106.

Pope, S.B., 2003. Turbulent flows. Cambridge University Press, Cambridge (UK).

Pui, D.Y.H., Romay–Novas, F., Liu, B.Y.H., 1987. Experimental study of particle deposition in bends of circular cross section. Aerosol Science and Technology 7, 301–315.

Ramamurthi, M., Strydom, R., Hopke, P.K., 1990. Assessment of wire and tube penetration theories using a $^{218}PoO_X$ cluster aerosol. Journal of Aerosol Science 21, 203–211.

Symonds, J.P.R., Olfert, J.S., Reavell, K.S.J., 2007a. Sampling line efficiency measured with a real time particulate size spectrometer. AAAR 26th Annual Conference, Reno, Nevada Poster presentation, September 24–28.

Symonds, J.P.R., Reavell, K.S.J., Olfert, J.S., Campbell, B.W., Swift, S.J., 2007. Diesel soot mass calculation in real–time with a differential mobility spectrometer. Journal of Aerosol Science 38, 52–68.

Tsai, C.J., Pui, D.Y.H., 1990. Numerical study of particle deposition in bends of a circular corss–section laminar flow regime. Aerosol Science and Technology 12, 813–831.

Wang, J., Flagan, R.C., Seinfeld, J.H., 2002. Diffusional losses in particle sampling systems containing bends and elbows. Journal of Aerosol Science 33, 843–857.

Wells, A.C., Chamberlain, A.C., 1967. Transport of small particles to vertical surfaces. British Journal of Applied Physics 18, 1793–1799.

## Figure Captions

**Fig. 1.** Schematic diagram of experimental set up. $L_{base}$/$L_1$, $L_2$, $L_3$ and $L_4$ are total length of sampling tubes between the manifold and DMS500; the tube length between the four–way switching system and the DMS500 was 0.30 m.

**Fig.2.** Effect of various lengths of sampling tubes on a typical diesel car exhaust emissions; figure represents cases $Car_1$ and $Car_2$.

**Fig. 3.** Size dependent measured and modelled penetration in **sampling tube $L_2$** for (a) $Car_2$ and $Car_3$ ($P$ = 160 mb, $T_a$ = 8.2 ºC, $Q$ = 2.5 slpm, $R_e$ = 461), (b) Cand and $Salt_1$ ($P$ = 160 mb, $T_a$ = 26 ºC, $Q$ = 2.5 slpm, $R_e$ = 461), (c) $Salt_2$ and $Salt_3$ ($P$ = 250 mb, $T_a$ = 26 ºC, $Q$ = 8 slpm, $R_e$ = 1409), and (d) average of (a) and (b). Acronyms $P$, $T_a$, $Q$ and $R_e$ represent the sample line pressure, ambient temperature, sample flow rate and Reynolds number, respectively. Further descriptions of all cases plotted in Figs. a–d are described in Table 1.

**Fig. 4.** Size dependent measured and modelled penetration in **sampling tube $L_3$** for (a) $Car_2$ and $Car_3$ ($P$ = 160 mb, $T_a$ = 8.2 ºC, $Q$ = 2.5 slpm, $R_e$ = 461), (b) Cand and $Salt_1$ ($P$ = 160 mb, $T_a$ = 26 ºC, $Q$ = 2.5 slpm, $R_e$ = 461), (c) $Salt_2$ and $Salt_3$ ($P$ = 250 mb, $T_a$ = 26 ºC, $Q$ = 8 slpm, $R_e$ = 1409), and (d) average of (a) and (b). Further descriptions of all cases plotted in Figs. a–d are described in Table 1.

**Fig. 5.** Size dependent measured and modelled penetration in **sampling tube $L_4$** for (a) $Car_2$ and $Car_3$ ($P$ = 160 mb, $T_a$ = 8.2 ºC, $Q$ = 2.5 slpm, $R_e$ = 461), (b) Cand and $Salt_1$ ($P$ = 160 mb, $T_a$ = 26 ºC, $Q$ = 2.5 slpm, $R_e$ = 461), (c) $Salt_2$ and $Salt_3$ ($P$ = 250 mb, $T_a$ = 26 ºC, $Q$ = 8 slpm, $R_e$ = 1409), and (d) average of (a) and (b). Further descriptions of all cases plotted in Figs. a–d are described in Table 1.

## Tables

**Table 1.** Summary of experimental and operating conditions.

| Cases | Aerosol Source | Place of Sampling | Length of Sampling tubes used | Sampling conditions |
|---|---|---|---|---|
| $Car_1$ | Diesel car | 50 cm away from exhaust tail pipe | $L_{base}$ | Particle size range 5–2738 nm, Sample line pressure 160 mb Ambient Temperature 8.2 °C Sample flow rate 2.5 slpm Reynolds number ($R_e$) = 461 |
| $Car_2$ | Diesel car | 50 cm away from exhaust tail pipe | $L_1$, $L_2$, $L_3$ and $L_4$ | |
| $Car_3$ | Diesel car | At the exit (i.e., 10 cm away from exhaust tail pipe) | $L_{base}$, $L_2$, $L_3$ and $L_4$ | |
| Cand | Candle | Candle flame 15 cm below the manifold inlet | $L_{base}$, $L_2$, $L_3$ and $L_4$ | Particle size range 5–2738 nm Sample line pressure 160 mb Indoor Temperature 26 °C Sample flow rate 2.5 slpm $R_e$ = 461 |
| $Salt_1$ | Nebulised NaCl(aq) | Generated at 2 bar pressure | $L_{base}$, $L_2$, $L_3$ and $L_4$ | |
| $Salt_2$ | Nebulised NaCl(aq) | Generated at 2 bar pressure | $L_{base}$, $L_2$, $L_3$ and $L_4$ | Particle size range 5–1000 nm Sample line pressure 250 mb Indoor Temperature 26 °C Sample flow rate 8 slpm $R_e$ = 1409 |
| $Salt_3$ | Nebulised NaCl(aq) | Generated at 0.5 bar pressure | $L_{base}$, $L_2$, $L_3$ and $L_4$ | |

**Figure 1.ppt**

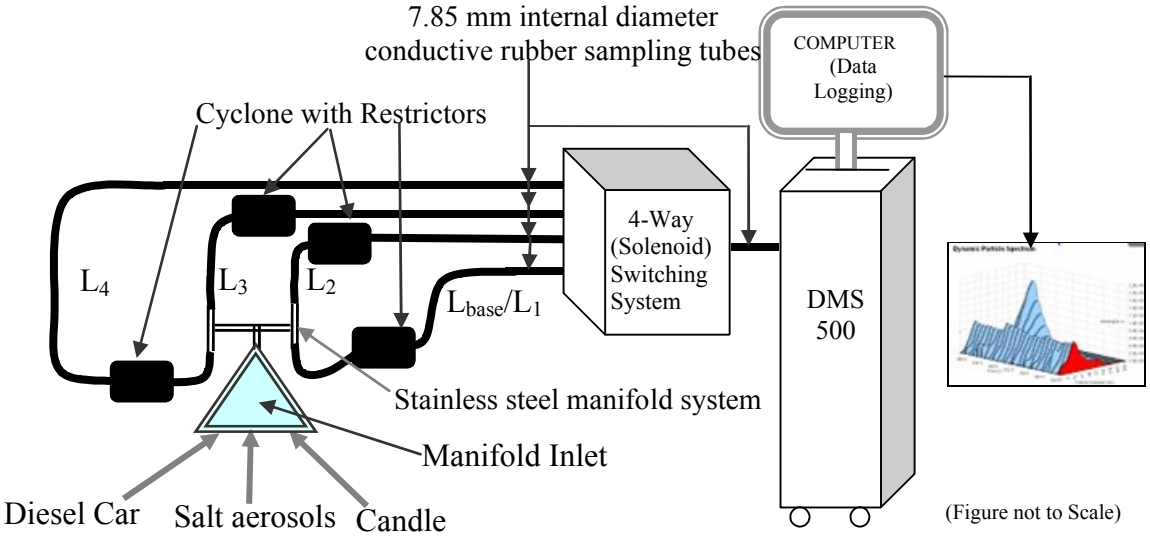
7.85 mm internal diameter
conductive rubber sampling tubes
COMPUTER
(Data
Logging)
Cyclone with Restrictors
4-Way
(Solenoid)
Switching
System
DMS
500
L4
L3
L2
Lbase/L1
Stainless steel manifold system
Manifold Inlet
Diesel Car
Salt aerosols
Candle
(Figure not to Scale)

**Figure 2.ppt**

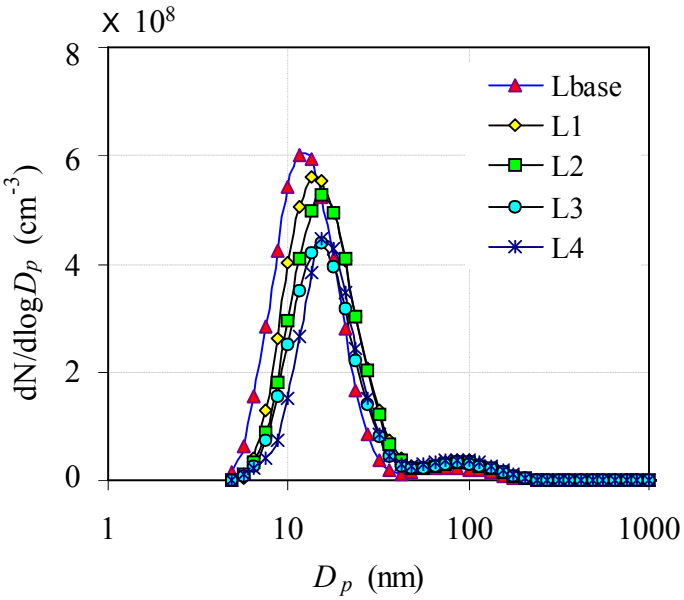

**Figure 3_For L2.ppt**

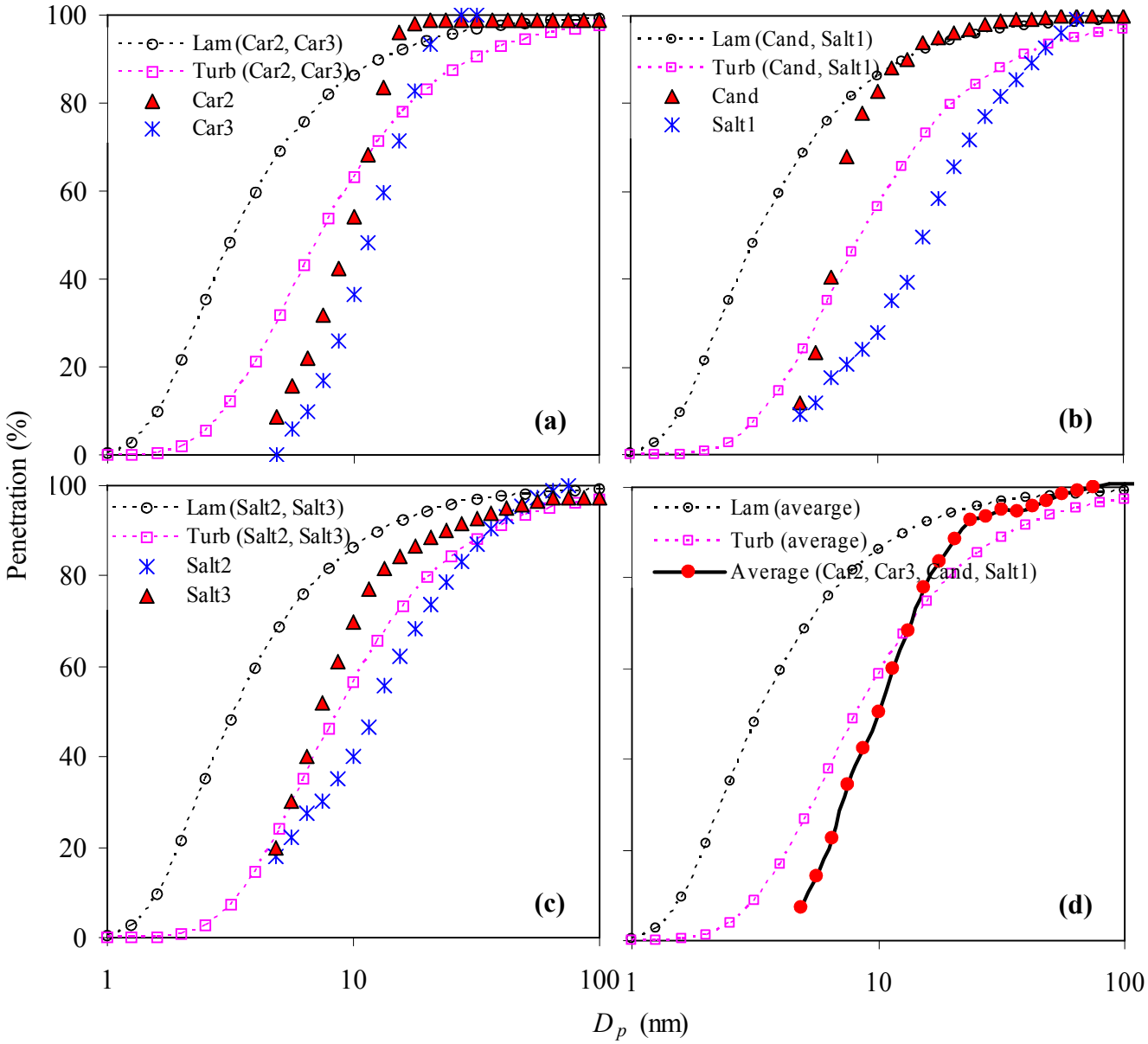

Figure 4_For L3.ppt

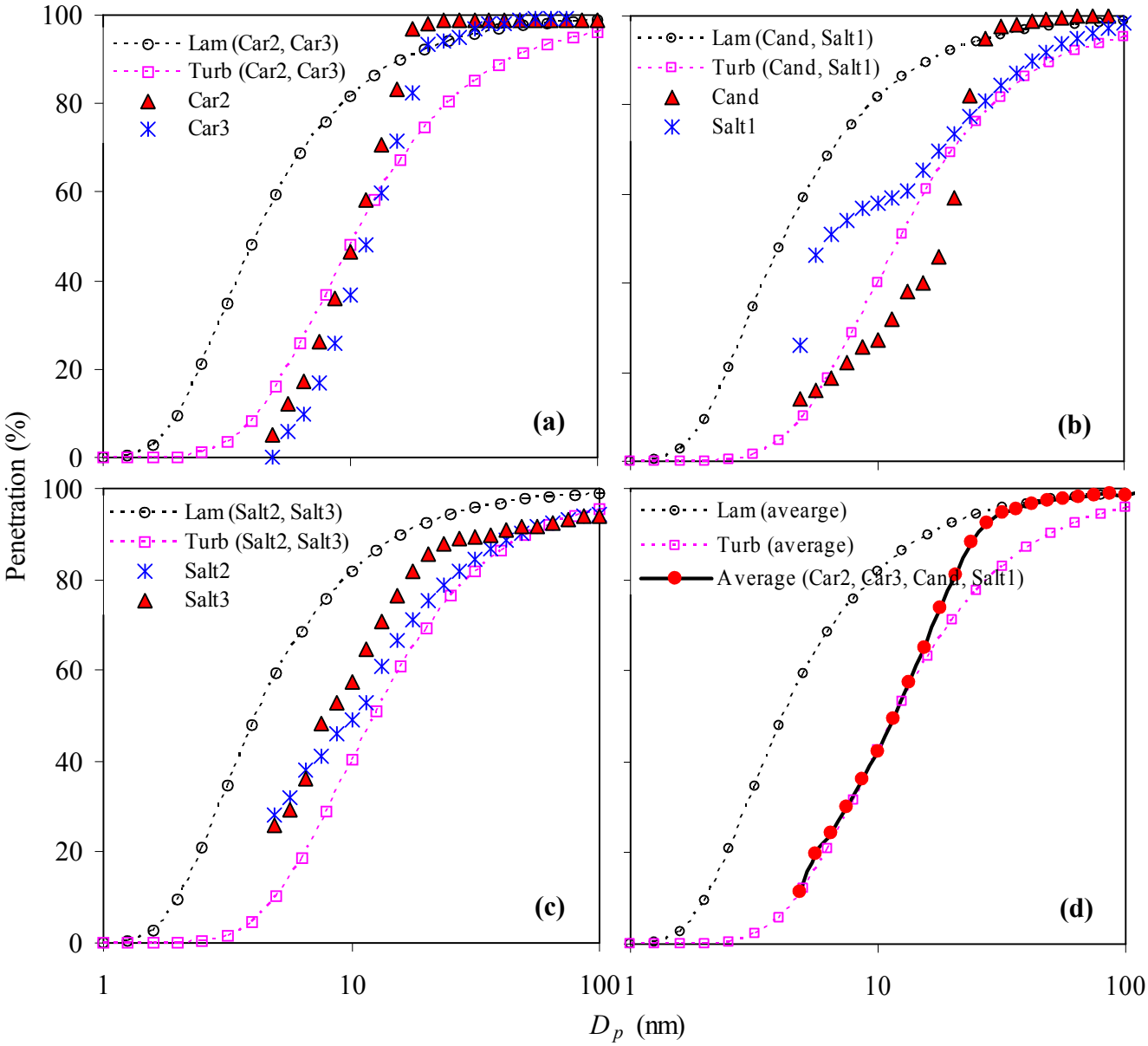

Figure 5_For L4.ppt